International Immunopharmacology 77 (2019) 105918

Contents lists available at ScienceDirect

International Immunopharmacology

journal homepage: www.elsevier.com/locate/intimp

1-Methylnicotinamide attenuates lipopolysaccharide-induced cognitive deficits via targeting neuroinflammation and neuronal apoptosis

Rong-hao Mu, Yuan-zhi Tan, Li-li Fu, Mohammad Nazmul Islam, Mei Hu, Hao Hong*, Su-su Tang*

Department of Pharmacology, and Jiangsu Key Laboratory of Drug Discovery for Metabolic Diseases, China Pharmaceutical University, Nanjing 210009, China

ARTICLE INFO

Keywords:
1-Methylnicotinamide
Lipopolysaccharide
Cognition deficits
Neuroinflammation
Neuronal apoptosis

ABSTRACT

Alzheimer's disease (AD) is a neurodegenerative disease that affects cognition and behavior. The neuroinflammatory response in the brain is an important pathological characteristic in AD. In this study, we investigated the neuroprotective effects of 1-Methylnicotinamide (MNA), known as the main metabolite of nicotinamide, on reducing lipopolysaccharide (LPS)-induced cognitive deficits via targeting neuroinflammation and neuronal apoptosis. We found that the mice treated with LPS exhibited cognitive deficits in the novel object recognition, Morris water maze and Y-maze avoidance tests. However, intragastric administration of MNA (100 or 200 mg/kg) for 3 weeks significantly attenuated LPS-induced cognitive deficits in mice. Importantly, MNA treatment suppressed the protein expression of nuclear factor-kappa B p65 (NF-κB p65), pro-inflammatory cytokines (TNF-α, IL-6) and decreased the activation of microglia and astrocytes in the hippocampus and frontal cortex of LPS-induced mice. In addition, MNA treatment suppressed neuronal apoptosis by reducing the number of TUNEL-positive cells, caspase-3 activation and increasing the level of Bcl-2/Bax ratio in the hippocampus and frontal cortex. These findings indicate that MNA could be a potential neuroprotective drug in neurodegenerative diseases such as AD.

1. Introduction

Alzheimer's disease (AD) is a gradually progressive neurodegenerative disorder characterized by cognitive impairment and dementia [1,2]. Neuroinflammation is an important pathological characteristic in Alzheimer's disease and other neurodegenerative diseases [3] and influences cognition and neuronal plasticity [4]. Particularly, brain-resident non-neuronal cells such as microglia are involved in the regulation of inflammatory responses through activation of immune components at the molecular level such as the pro-inflammatory cytokines and the complement system [5,6]. Although activation of glial cells is requisite for host defense and maintaining homeostasis, over-activation of glial cells, such as microglia and astrocytes, contribute to neuron death and neurodegenerative disorders [7]. Previous studies have shown that intraperitoneal injection of lipopolysaccharide (LPS) which is an endotoxin from gram-negative bacteria leads to microglial over-activation and induces neuroinflammation [8], memory impairment and neuronal apoptosis [9].

1-Methylnicotinamide (MNA) is the main metabolite of the amide form of vitamin B3 which is known as nicotinamide (NA) [10,11]. The N-methylation of pyridine compound NA by nicotinamide N-methyltransferase (NNMT), an enzyme found predominantly in the liver, leads to the formation of MNA [12]. Evidence has shown the biological activity of MNA, an activator of prostacyclin production, can regulate both thrombotic and inflammatory processes in the cardiovascular system [13]. Oral administration of MNA can ameliorate free fatty acid-bound albumin-induced oxidative stress, inflammation, apoptosis, necrosis, and fibrosis in the kidneys of mice [14]. Furthermore, MNA plays a protective role against concanavalin A-induced liver injury via inhibiting the release of pro-inflammatory cytokines IL-4 and TNF-α. It has been reported that MNA may have a beneficial role in degenerative diseases as it inhibits the transport of choline out of the central nervous system and increases the levels of acetylcholine in the brain tissue [15,16]. MNA treatment also increase the uptake of serotonin with a normalizing effect on spontaneous neurotransmitter release in diabetic brain synaptosome [17]. The previous studies have demonstrated that MNA provides neuroprotection to cerebellar granule cells against homocysteine and glutamate excitotoxicity [18,19]. However, the exact mechanism of MNA in neuroprotective effect remains unclear. The aims of the present study were to investigate the neuroprotective effects of MNA on cognitive impairment in LPS-induced mice and the possible underlying mechanism by detecting inflammatory factors and neuronal apoptosis-related proteins.

* Corresponding authors.
E-mail addresses: honghao@cpu.edu.cn (H. Hong), tang_susu@126.com (S.-s. Tang).

https://doi.org/10.1016/j.intimp.2019.105918
Received 11 July 2019; Received in revised form 13 September 2019; Accepted 13 September 2019
Available online 19 October 2019

2. Materials and methods

2.1. Animals

Male SPF grade ICR mice (weighing 22–24 g, 3-month old) provided by the Medical Center of Yangzhou University (Yangzhou, China). The animal approval number was SCXK: 2017-0001. Animals were housed under conditions of a temperature of 20–24 °C, a humidity of 55 ± 5%, and a 12 h/12 h cycle of illumination, during which animals were free to eat and drink. The experiment was started one week after the animals were adapted for feeding. Animal experiments were organized and carried out in accordance with the guidelines of the National Institutes of Health Guide and Care of Laboratory Animals. The methods were endorsed by the Animal Care and Use Committee of China Pharmaceutical University. The animal approval number for experiments of China Pharmaceutical University was SYXK: 2016-0011.

2.2. Drugs and reagents

MNA was purchased from Tokyo Chemical Industry Co., Ltd. (Tokyo, Japan) and dissolved in sterile saline. LPS was purchased from Sigma Aldrich (St. Louis, MO, USA), dissolved in sterilized saline water and administered intraperitoneally (i.p.) with a dose of 250 μg/kg for 7 days [20]. The antibodies were purchased from the following companies: anti-cleaved caspase-3, anti-IL-6 and anti-Bcl-2 were from Cell Signaling Technology, Inc. (Massachusetts, USA); anti-Bax and anti-TNF-α were from Santa Cruz Biotechnology, Inc. (Heidelberg, Germany); anti-GFAP and anti-NeuN were from Abcam, Inc. (Cambridge, USA); anti-NF-κB p65 was from Cell Signaling Technology, Inc. (Massachusetts, USA); anti-Iba1 was from Wako Pure Chemical Industries, Ltd. (Osaka, Japan); Histone H3, β-actin and secondary antibodies were from Bioworld Technology Co., Ltd. (Minnesota, USA). The nucleoprotein extraction kit was from Sangon Biotech Co., Ltd. (Shanghai, China), and streptavidin-biotin complex (SABC) immunohistochemistry kit was from Boster Biotechnology Co., Ltd. (Wuhan, China).

2.3. Drug treatments

Experimental mice were divided randomly into five groups: Veh + Veh, Veh + LPS, LPS + MNA 50 mg/kg, LPS + MNA 100 mg/kg, and LPS + MNA 200 mg/kg. Mice in each group were given sterile saline or MNA (50, 100, 200 mg/kg) intragastrically (i.g.) for three weeks, and LPS (250 μg/kg, i.p.) was performed in the third week [21–23] except for the Veh + Veh group. All animals were intraperitoneally injected with LPS or sterile saline 30 min before administration of MNA or sterile saline. All drugs were administered at a volume of 10 ml/kg body weight. Then, mice were subjected to behavioral trials, such as open field, novel object recognition (NOR), Morris water maze (MWM) and Y-maze avoidance tests, to evaluate and analyze the memory and learning functions. Brain tissues of mice were used for biochemical analysis. Animal groups and the experimental schedule are schematically depicted in Fig. 1A.

2.4. Open field test (OFT)

OFT is the most common procedure that allows to study or evaluate locomotor activity and behavior of different mice [24]. The open field test was carried out in a quiet environment free of external influences. In this test, a plastic box with dimensions of 50 cm × 50 cm × 40 cm was divided into 144 squares. The mouse was gently placed in any corner square facing the wall and allowed to freely explore the box. The total distance covered by mice was recorded within 5 min. The box was cleaned with 70% ethanol to eliminate the odor before the next test.

2.5. Novel object recognition (NOR) test

NOR test is used to detect the memory and learning function [25]. This test is accomplished within three days, that is habituation day, training day and testing day [26]. The first day was the habitual stage and the mice were allowed to move freely in a rectangular plastic box (50 cm × 50 cm × 40 cm). On the second day, the mice were allowed to explore two identical objects and the exploration time recorded in 5 min. On the third day, one of the objects was changed to a new object (different color and shape), and the mice also explored for 5 min. The time spent exploring (less than 2 cm away from the object and touched the object with the mouth, nose, or paw) the two objects within 5 min was recorded by the computer. After each mouse completed the test, 70% ethanol was used to clean the urine and excrement so as not to affect the next mouse test. The exploring time for the same objects A and B during the familiar period was defined as EA1 and EA2; in the testing trial with the investigative time for original object A and novel object B was EA and EB. The discrimination index was determined by performing the following calculation: (EB − EA)/(EB + EA).

2.6. Morris water maze (MWM) test

To assess spatial learning and memory, the MWM test is widely used [27,28]. The mice were individually placed in a round pool with a 1.2 m diameter, 0.5 m height and filled with water to a 0.3 m depth at a temperature of 25 °C. An escape platform with a diameter of 9 cm was placed at the midpoint of any quadrant of the pool. During the entire test, this pool was placed in a quiet room with visual cues. The test consisted of five days training period with visible and hidden platform. The escape platform always stayed at a fixed position during the entire duration of training (5 days). On every trial, mice were put into the pool with facing the pool wall. The visible platform training sessions were done on day 1 and day 2. The invisible platform training sessions were done from day 3 to day 5 and the probing trial was conducted on day 6. During each trial, every mouse was exposed to four quadrants and there was a 1-hour time interval between trials. During the first 2 days, the platform, bundled with a small flag, was fixed 1 cm below the surface of the water. From day 3 to day 5, the small flag was removed but the position of the platform remained the same. In this case, the baseline differences in vision and motivation were assessed using the visible platform test, and the spatial learning in the determination of memory retention to find the platform was assessed using the hidden escape platform test. In MWM test, from day 1 to day 5, each test is last 90 s. If the mouse finds the platform and stay there for 10 s, the test can end early. On the other hand, if the mouse did not find the escape platform in 90 s, it would be physically placed on the platform to learn for 30 s. On the final day (day 6), during the probing test, the mice were allowed to swim for 90 s while the platform is taken away. The trend of the mice to search for the platform is measured by the time spent in the target quadrant where the escape platform was previously located. The number of times in which each individual mouse passed the escape platform location was recorded and processed using video tracking device and computer-equipped analytics management system (Viewer 2 Tracking Software, Ji Liang Instruments, China).

2.7. Y-maze avoidance test

Y-maze avoidance test described [29] elsewhere was conducted for 2 days. On the first day, each mouse was placed in one of the three compartments and allowed to move freely for 5 min. After 5 min, the electrical shocks (2 Hz, 125 ms, 10 V) in two compartments were made available through a stainless-steel mesh floor whereas a compartment was kept free from electric shock but provided with light sources as hints to enter. The same procedure was conducted on each mouse for 10 times. Once the mouse entered the light source of the area and stayed for 30 s, then the session was terminated. If the mouse went to the

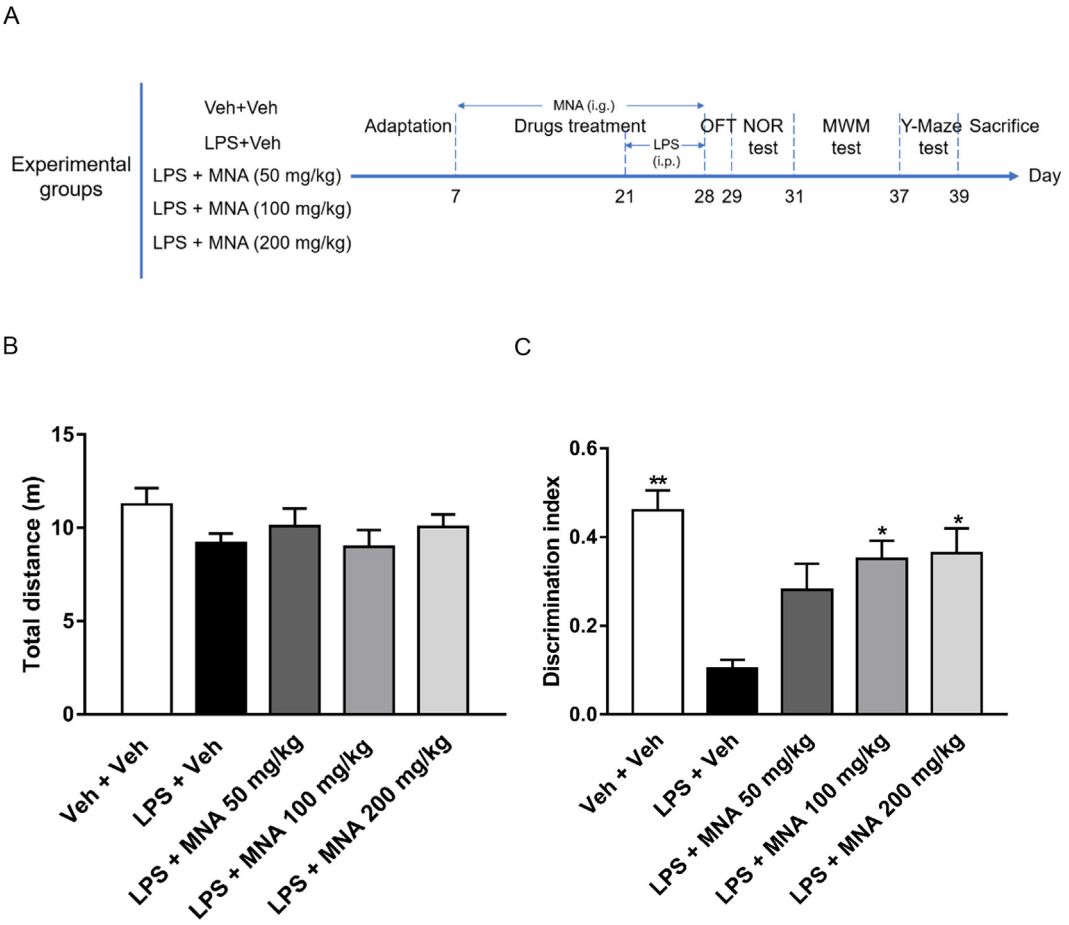

Fig. 1. Effects of MNA on LPS-treated mice in the locomotor activity and NOR tests. (A) Animal groups and the schedule of the experiment. (B) The total distance in OFT. (C) The discrimination index in NOR test. The discrimination index was determined by performing the following calculation: (EB − EA)/(EB + EA). Values shown were expressed as mean ± SEM; n = 12 mice/group. *$P < 0.05$, ** $P < 0.01$ vs. LPS + Veh.

shock-free compartment on the first occasion, it was noted as a right selection. If not, tenderly guided the mice to the compartment and stayed for 30 s. On the second day, testing trial was conducted similar to that of day 1 but with no adaptation phase. The number of correct choices and latency to enter the shock-free compartment were recorded on the second day.

2.8. Tissue preparation and immunohistochemistry (IHC)

For tissue preparation, mice were anaesthetized and transcardially perfused with 60 ml PBS followed by 4% paraformaldehyde in PBS. After this, the brain was removed and subsequently submerged into 4% paraformaldehyde at a temperature of 4 °C for 24 h and cryoprotected in 30% sucrose solution for an additional period of 24 h prior to further treatment. Finally, the brain was embedded into an optimal cutting temperature compound (Tissue-Tek, Torrance, CA) and cryosectioned (30 μm). Brain sections were washed using PBS (3 × 5 min) followed by heating using a water bath with for 4 h at 60 °C with 0.3% Triton X-100. After this, the brain sections were treated with 3% H_2O_2 at room temperature for 30 min. Following the washing with PBS (3 × 5 min), sections were blocked with 5% BSA for 30 min and incubated in anti-Ibal (1:1000) and anti-NeuN (1:500) primary antibody diluted in 5% BSA overnight at 4 °C. The following day, brain sections were washed again with PBS (3 × 5 min) and further incubated with biotinylated mouse anti-rabbit IgG for 40 mins at 37 °C. After further washing in PBS (3 × 5 min, 37 °C), slices were incubated with streptavidin-biotin complex (20 min, 37 °C) and washed with PBS again (4 × 5 min). Diaminobenzidine (DAB) was applied as the ultimate chromogen for protein detection followed by gradient dehydration (70% ethanol for 5 mins then 95% ethanol for another 5 mins and finally 100% ethanol for 2 × 5 min and xylene for 2 × 5 min). Sections were then covered using Dibutyl Phthalate Xylene (DPX) fixation solution and cover glass. Finally, the sections were observed with a light Microscope (Leica Microsystems AG, Germany) at a constant magnification (×200). The amount of microglia in the hippocampus was measured, followed by the microglial-positive area. These values were used to generate the ratio of microglial staining to the hippocampal area (% area occupied). The mean values from all the 4 sections of the brain of each mouse were used in statistical analysis.

2.9. Immunofluorescence (IF)

The brain slice was taken out and immersed in a well plate containing PBS to rewarm and wash (3 × 10 min). Brain slices were incubated with PBS diluted 3% H_2O_2 for 0.5 h to inactivate endogenous catalase, and then washed with PBS. Slices were removed and immersed in a solution containing PBST for 20 min (diluted with PBS 0.3% Triton X-100 or PBST), and washed with PBS again (3 × 5 min). Slices were blocked by 5% serum at room temperature for 60 min. Then, serum was discarded, and the primary antibody (anti-GFAP antibody 1:500) diluted by serum was added to incubate the slices overnight at 4 °C. The second day, the primary antibody was discarded and the brain slices were washed with PBS (3 × 5 min), and then incubated with PBST diluted fluorescein-labeled secondary antibody (Alexa Fluor 488 labeled anti-rabbit IgG: 1:200) at room temperature in the dark for 60 min. Brain slices were washed for 15 min in the dark, DAPI staining

(5–10 min), and washed with PBS (3 × 5 min). Finally, the slices are transferred to glass slides, and the fluorescent anti-quenching agent was added dropwise to cover the slide. The cells were observed under a fluorescence microscope and photographed.

2.10. Extraction of total and nuclear protein

Mouse hippocampus and frontal cortex were chopped into small pieces and homogenized in ice-cold RIPA (50 mM Tris-HCl (pH 7.4), 150 nM NaCl, 1 mM PMSF, 1 mM EDTA, 1% Triton X-100, 1% sodium deoxycholate, 0.1% SDS). The dissolved proteins were collected from the supernatant after centrifugation at 4 °C, 12000 rpm for 15 min. Protein concentration in the supernatant was determined using a BCA protein assay kit under the manual guidelines (Beyotime Biotechnology, Jiangsu, China). The extract was used to assess the protein expression of pro- or cleaved caspase-3, Bax, Bcl-2, IL-6, TNF-α and β-actin.

Nuclear proteins were extracted using the nucleoprotein extraction kit from Sangon Biotech, China. Firstly, the mouse hippocampus and frontal cortex were minced and homogenized in the ice-cold hypotonic buffer, which was made up of 0.5% phosphatase inhibitor, 1% PMSF and 0.1% DL-Dithiothreitol (DTT). After this, the solution was centrifuged at a temperature of 4 °C, 3000 rpm for 5 min. The supernatant was disposed and the precipitate was washed in hypotonic buffer and centrifuged at 5000 rpm for 5 min at 4 °C. At the end, 0.2 ml lysis buffer (containing 0.5% phosphatase inhibitor, 1% PMSF and 0.1% DTT) was added into the precipitate, chilled for 20 min and then centrifuged at 15000 rpm for 10 min at 4 °C. The supernatant nuclear protein extract was assessed the expression of NF-κB p65and Histone H3.

2.11. Western blot (WB) analysis

For assessing the protein expression, protein extracts were separated by SDS-polyacrylamide gel electrophoresis and then transferred onto polyvinylidene difluoride (PVDF) membranes. The membranes were blocked with 5% (w/v) skim milk to reduce non-specific binding and incubated at 4 °C overnight with respective primary antibodies for TNF-α (1:500), IL-6 (1:1000), caspase-3 (1:1000), Bcl-2 (1:1000), Bax (1:500); β-actin (1:5000) was used as the control. For NF-κB p65 (1:1000), Histone H3 (1:500) was used as the control. After over-night of incubation, membranes were washed with Tris buffer saline-tween 20 (TBST) and incubated with a horseradish peroxidase-conjugated secondary antibody (1:5000) for 2 h at room temperature. Enhanced chemiluminescence detection reagents and a gel imaging system (Tanon Science & Technology Co, Ltd., China) were used to visualize the immunoreactive bands.

2.12. TUNEL staining

Terminal deoxynucleotidyl transferase (TdT)-mediated dUTP nick-end labelling (TUNEL) staining is used to identify nuclei with fragmented DNA (features of apoptotic cells) by utilizing the in-situ cell death detection kit (Roche, Germany). Brain sections were fixed in 4% PFA for 20 min at the temperature of 37 °C followed by washing with PBS (pH 7.4) for 30 min at 37 °C. The sections were then incubated in 0.1% Triton X-100, 0.1% sodium citrate solution newly prepared for 2 min on ice. Afterwards, the TUNEL concoction was added onto the brain sections and incubated in a humidified chamber for 60 min at 37 °C. After this, they were washed in PBS (pH 7.4) (2 × 5 min) at 37 °C. Sections were then incubated for 10 min in dark for DAPI staining. The cells were observed using a fluorescence microscope under a precise magnification (×200) (Leica Microsystems AG, Germany). TUNEL-positive cells were identified by the co-localization of both the TUNEL signal and DAPI. The apoptotic bodies were quantified and then expressed as a percentage of the overall number of cells examined. The mean values from all the 4 brain sections of each mouse were used in statistical analysis.

2.13. Statistical analysis

The results were expressed as mean ± standard error of mean (SEM). SPSS software (version 20.0; IBM, Armonk, NY) was used for statistical analyses. In the MWM test, group differences were analyzed by a two-way repeated measure analysis of variance (ANOVA) with “days” as the within-subject factor and “group” as the between-subject factor. All other data were analyzed by a one-way ANOVA followed by a Dunnett's post-hoc analysis for multiple comparisons. $P < 0.05$ was considered statistically significant.

3. Results

3.1. MNA improves LPS-induced memory impairment in mice

After the administration of drugs, we firstly evaluated the locomotor activity of mice. In OFT, the total distance of each group had no difference, suggesting the drugs have no effect on spontaneous locomotor activity in mice ($F [4,55] = 1.264$, $P > 0.05$; Fig. 1B). In NOR test, compared with the Veh + Veh group, the discrimination index in the Veh + LPS group was significantly decreased ($F [4,55] = 3.818$, $P < 0.01$; Fig. 1C), and intragastric administration of MNA significantly increased the discrimination index (MNA 100 mg/kg: $P < 0.05$, MNA 200 mg/kg: $P < 0.05$; Fig. 1C).

Previous study in our laboratory has demonstrated that injection of LPS leads to learning and memory deficits [30]. In this study, the MWM results showed that mice in each group exhibited similar escape latency, indicating that there was no difference in vision or basal motivation among all groups (4 trials/day for 2 days; effect of day, $F [4, 535] = 3.743$, $P < 0.01$; effect of Group, $F [4, 535] = 0.9809$, $P > 0.05$; effect of group-by-day interaction, $F [4, 535] = 0.0508$, $P > 0.05$; Fig. 2A). In the hidden platform training, compared with the Veh + Veh group, the latency in the Veh + LPS group was increased. After the MNA administration, the latency was reduced but there was no statistical difference (4 trials/day for 3 days; effect of day, $F [4, 775] = 5.230$, $P < 0.01$; effect of group, $F [4, 775] = 1.044$, $P > 0.05$; effect of group-by day interaction, $F [4, 775] = 0.0370$, $P > 0.05$; Fig. 2B). In the probe trial, compared with the Veh + Veh group, the percentage of target quadrant residence time ($F [4,55] = 5.229$, $P < 0.01$) and the number of escape platform crossing ($F [4,55] = 5.472$, $P < 0.01$) in the Veh + LPS group decreased significantly. Administration of MNA significantly increased the percentage of time in the target quadrant (MNA 100 mg/kg: $P < 0.05$; MNA 200 mg/kg: $P < 0.05$, Fig. 2D) and the number of escape platform crossing (MNA 100 mg/kg: $P < 0.05$; MNA 200 mg/kg: $P < 0.05$, Fig. 2E). Representative swimming trajectories of each group of mice in the space exploration experiment are shown in Fig. 2C.

The Results of Y-maze avoidance test showed that compared with the Veh + Veh group, the number of correct choices in the Veh + LPS group was significantly reduced ($F [4,55] = 0.4480$, $P < 0.01$), and the latency to enter the shock-free compartment significantly increased ($F [4,55] = 5.481$, $P < 0.01$). Administration of MNA significantly increased the number of correct choices (MNA 100 mg/kg: $P < 0.05$; MNA 200 mg/kg: $P < 0.05$; Fig. 2F) and reduced the latency of selecting the shock-free compartment (MNA 100 mg/kg: $P < 0.05$; MNA 200 mg/kg: $P < 0.05$; Fig. 2G).

3.2. MNA inhibits LPS-induced neuroinflammatory response in the hippocampus and frontal cortex

LPS stimulation can activate the NF-κB signaling pathway which plays a significant role in the regulation of neuroinflammation. Therefore, suppression of NF-κB signaling pathway can inhibit the release of inflammatory mediators [31]. In order to investigate whether

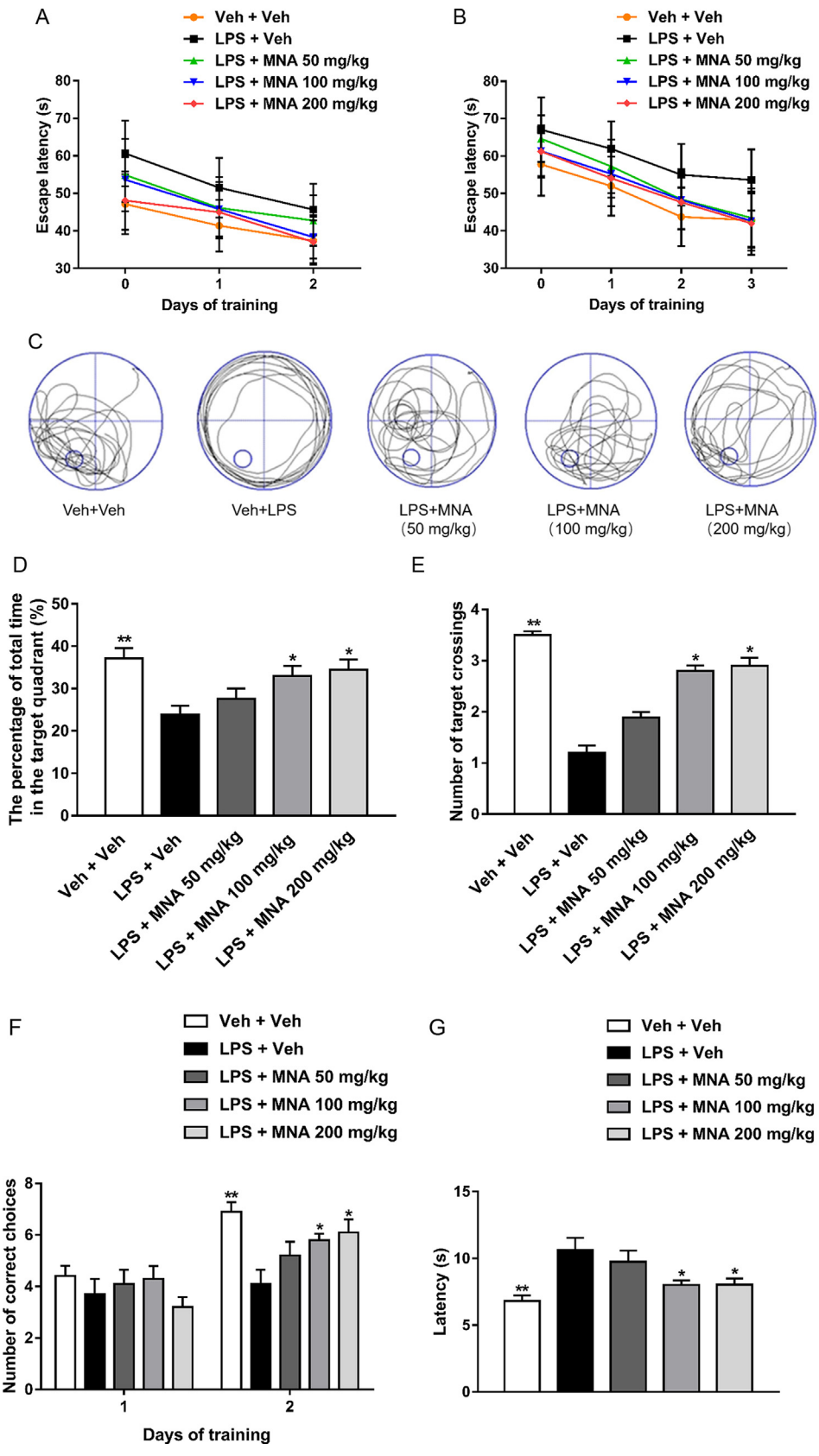

Fig. 2. MNA improves LPS-induced memory impairment in MWM and Y-maze tests. (A) The escape latency during the two days visible platform test. Day 0 indicates performance on the first trial and subsequent points represent an average of all daily trials. (B) The escape latency on hidden platform test. (C) A representative swimming path of mice. (D) The percentage of total time spent in the target quadrant. (E) The number of platform crossings during the probe trial test. (F) The number of correct choices in Y-maze test. (G) The latency to enter the shock-free part on Day 2 in Y-maze test. Values shown were expressed as mean ± SEM; n = 12 mice/group. * $P < 0.05$, ** $P < 0.01$ versus LPS + Veh.

MNA regulate the NF-κB signaling pathway in the brain of LPS-induced mice, we used western blot to detect the expression of NF-κB p65 in the hippocampal and frontal cortex nucleus of mice. We found that the nuclear expression of NF-κB p65 was significantly increased after injection of LPS in the hippocampus and frontal cortex of mice. (hippocampus: F [4,55] = 12.65, $P < 0.01$; frontal cortex: F [4,55] = 7.828, $P < 0.01$; Fig. 3A and B). But MNA treatment significantly attenuated these changes (hippocampus: MNA 100 mg/kg:

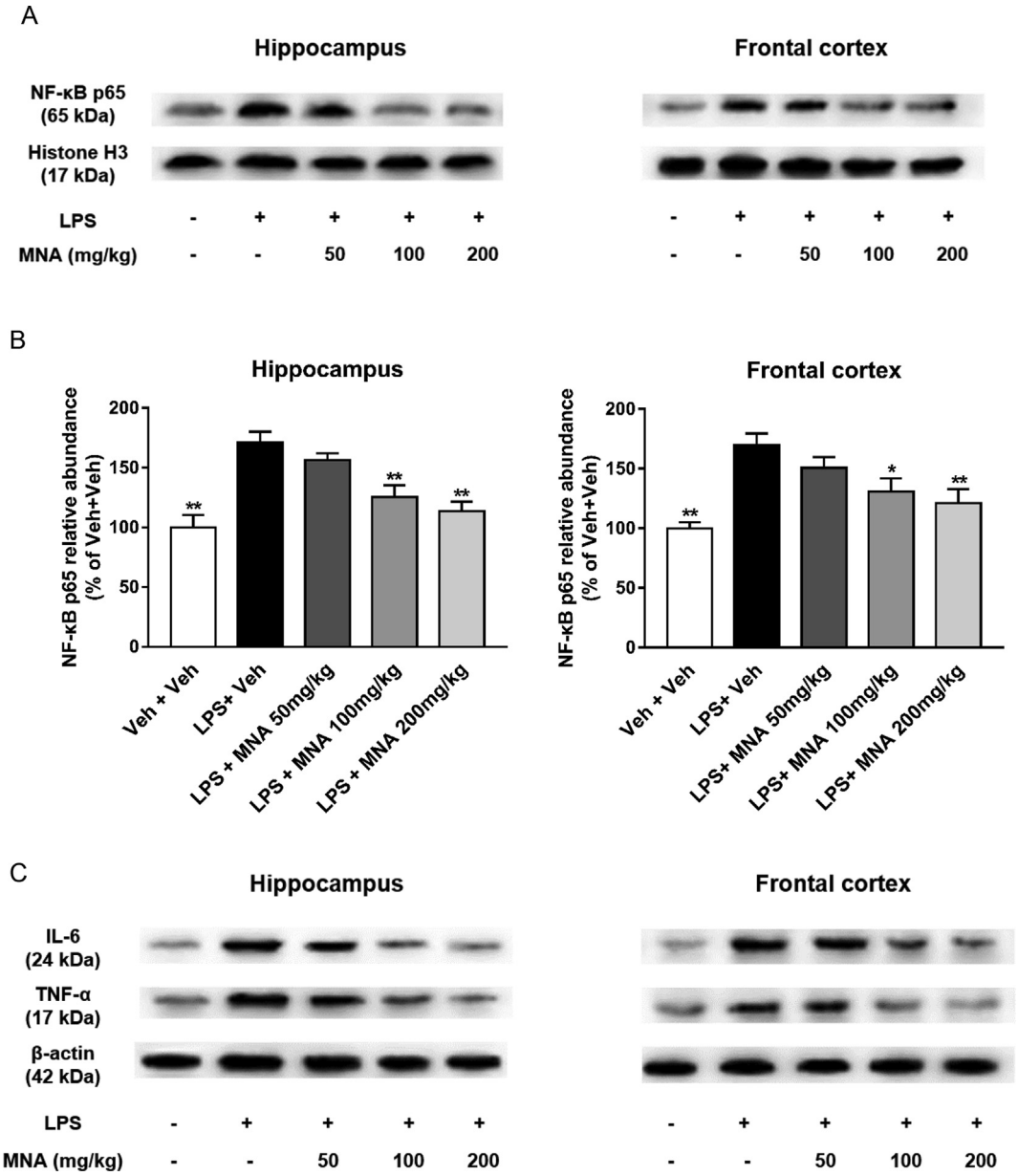

Fig. 3. MNA inhibits LPS-induced neuroinflammatory responses in the hippocampus and frontal cortex. (A) The expressions of NF-κB p65 in the hippocampus and frontal cortex were detected by WB. Histone H3 was used as a loading control. (B) Quantification of NF-κB level was expressed as the percentage of Veh + Veh group. (C) The expressions of IL-6 and TNF-α in the hippocampus and frontal cortex were detected by WB. β-actin was used as a loading control. Quantification of IL-6 (D) and TNF-α (E) levels were expressed as the percentage of Veh + Veh group. Values shown were expressed as mean ± SEM; n = 4 mice/group. * $P < 0.05$, ** $P < 0.01$ versus LPS + Veh.

$P < 0.01$; MNA 200 mg/kg: $P < 0.01$; frontal cortex: MNA 100 mg/kg: $P < 0.05$; MNA 200 mg/kg: $P < 0.01$; Fig. 3A and B). In addition, to investigate the effects of MNA on neuroinflammation, we used western blot to detect the expression of inflammatory factors in the hippocampus and frontal cortex of mice. The results showed that LPS significantly increased the expressions of IL-6 (hippocampus: F [4,55] = 8.588, $P < 0.01$; frontal cortex: F [4,55] = 7.760, $P < 0.05$; Fig. 3C, D) and TNF-α (hippocampus: F [4,55] = 9.715, $P < 0.01$; frontal cortex: F [4,55] = 5.595, $P < 0.01$; Fig. 3C and E). But MNA treatment significantly attenuated these changes (hippocampus: MNA 100 mg/kg: $P < 0.05$; MNA 200 mg/kg: $P < 0.01$ for IL-6 and TNF-α; frontal cortex: MNA 100 mg/kg: $P < 0.05$; MNA 200 mg/kg: $P < 0.05$ for IL-6 and TNF-α; Fig. 3C–E).

3.3. MNA inhibits LPS-induced glial cells activation in the hippocampus and frontal cortex

Activation of microglia and astrocytes are involved in the pathogenesis and progression of neurodegenerative diseases, such as Alzheimer's disease. To further investigate the effects of MNA on neuroinflammation, we detected the activation of microglia and astrocytes of mice in the hippocampus and frontal cortex by immunohistochemistry and immunofluorescence. The results showed that compared with the Veh + Veh group, the positive cells of Iba1 (microglial marker; hippocampus: F [4,55] = 27.04, $P < 0.01$; frontal cortex: F [4,55] = 6.085, $P < 0.01$; Fig. 4A and B) and GFAP (astrocytic marker; hippocampus: F [4,55] = 8.229, $P < 0.01$; frontal cortex: F [4,55] = 5.928, $P < 0.01$; Fig. 4C and D) were increased significantly in the hippocampus and frontal cortex after injection of

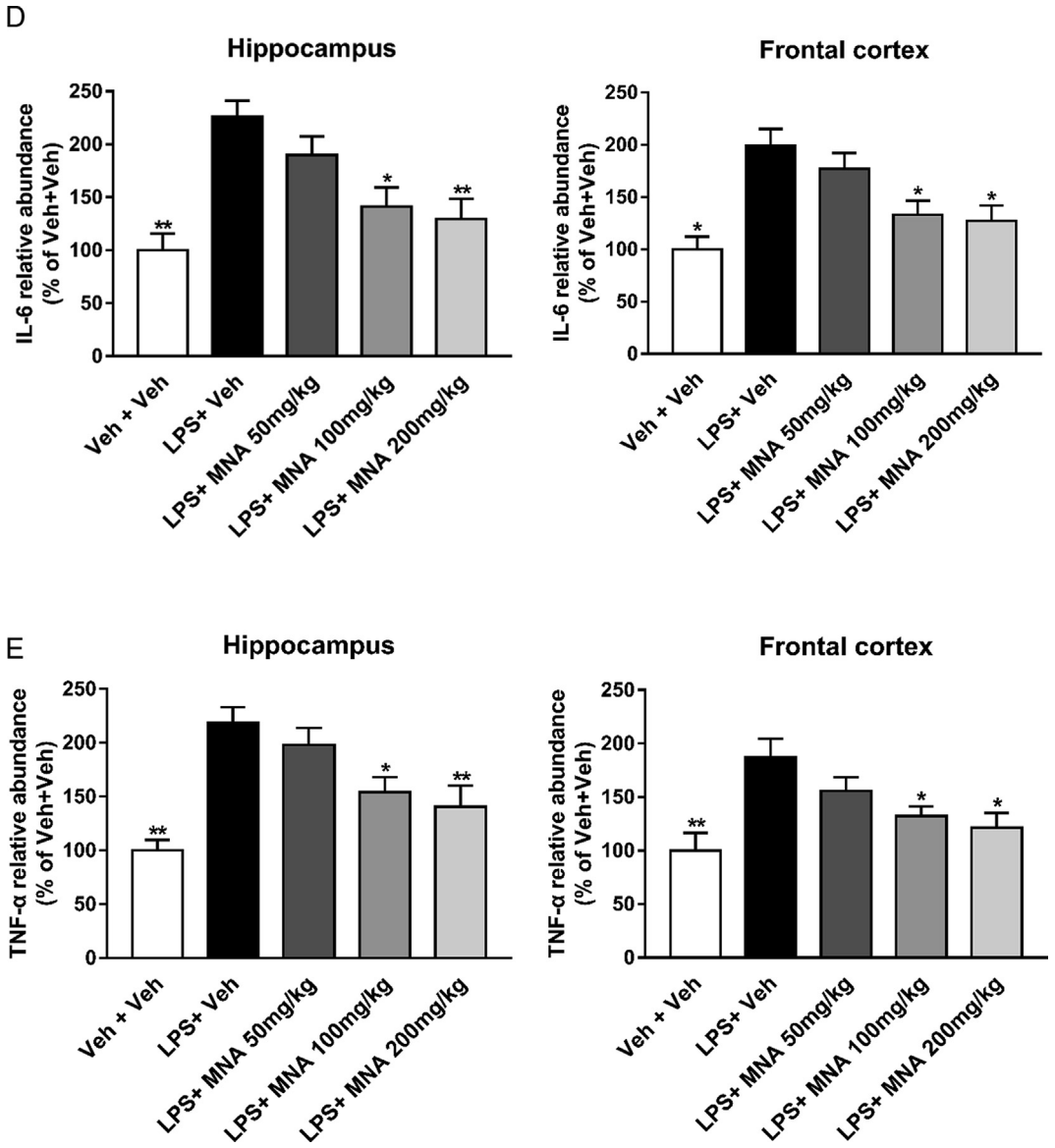

Fig. 3. (*continued*)

LPS. It indicated that LPS could promote activation of glial cells. In addition, administration of MNA significantly suppressed microglial and astrocytes activation (hippocampus and frontal cortex: MNA 100 mg/kg: $P < 0.05$; MNA 200 mg/kg: $P < 0.05$; Fig. 4B and D).

3.4. MNA inhibits LPS-induced neuronal apoptosis in the hippocampus and frontal cortex

To investigate the neuroprotective effects of MNA on neuronal apoptosis, we assessed apoptosis by TUNEL staining. As shown in Fig. 5, the number of TUNEL-positive cells in the hippocampal dentate gyrus (DG) and frontal cortex of the Veh + LPS group was significantly increased compared with the Veh + Veh group (hippocampus: $F[4,55] = 8.265$, $P < 0.01$; frontal cortex: $F[4,55] = 4.221$, $P < 0.01$; Fig. 5A and B), administration of MNA significantly reduced the number of TUNEL-positive cells (hippocampus and frontal cortex: MNA 100 mg/kg: $P < 0.05$; MNA 200 mg/ kg: $P < 0.05$; Fig. 5A and B). To investigate whether MNA treatment could prevent neuronal death against LPS neurotoxicity, we detected the expression of a neuronal marker NeuN in DG of hippocampus and frontal cortex by IHC. The results showed that MNA treatment significantly attenuated LPS-induced neuronal death (hippocampus: MNA 100 mg/kg: $P < 0.05$; MNA 200 mg/kg: $P < 0.01$; frontal cortex: MNA 100 mg/kg: $P < 0.05$; MNA 200 mg/kg: $P < 0.05$; Fig. 5C and D). In addition, we detected the expression of apoptosis-related proteins by Western blot. The results showed that the ratio of caspase-3 activation was significantly increased after LPS administration (hippocampus: $F[4,55] = 11.07$, $P < 0.01$; frontal cortex: $F[4,55] = 16.56$, $P < 0.01$; Fig. 5E and F), while the ratio of Bcl-2/Bax was decreased (hippocampus: $F[4,55] = 8.554$, $P < 0.01$; frontal cortex: $F[4,55] = 13.63$, $P < 0.01$; Fig. 5G and H). Treatment of MNA significantly attenuated these changes (hippocampus: and frontal cortex: MNA 100 mg/kg: $P < 0.05$; MNA 200 mg/kg: $P < 0.01$ for caspase-3, Fig. 5F; hippocampus: MNA 100 mg/kg: $P < 0.05$; MNA 200 mg/kg: $P < 0.01$ for ratio of Bcl-2/Bax; frontal cortex: MNA 100 mg/kg: $P < 0.01$; MNA 200 mg/kg: $P < 0.01$ for ratio of Bcl-2/Bax, Fig. 5G, H).

4. Discussion

In the present study, we investigated the neuroprotective effects of MNA in LPS-induced mice. Consistent with the previous findings, current study found systemic administration of LPS significantly impaired memory and learning function in mice. In MWM test, LPS-induced mice exhibited a significant decline in the amount of time spent in the target

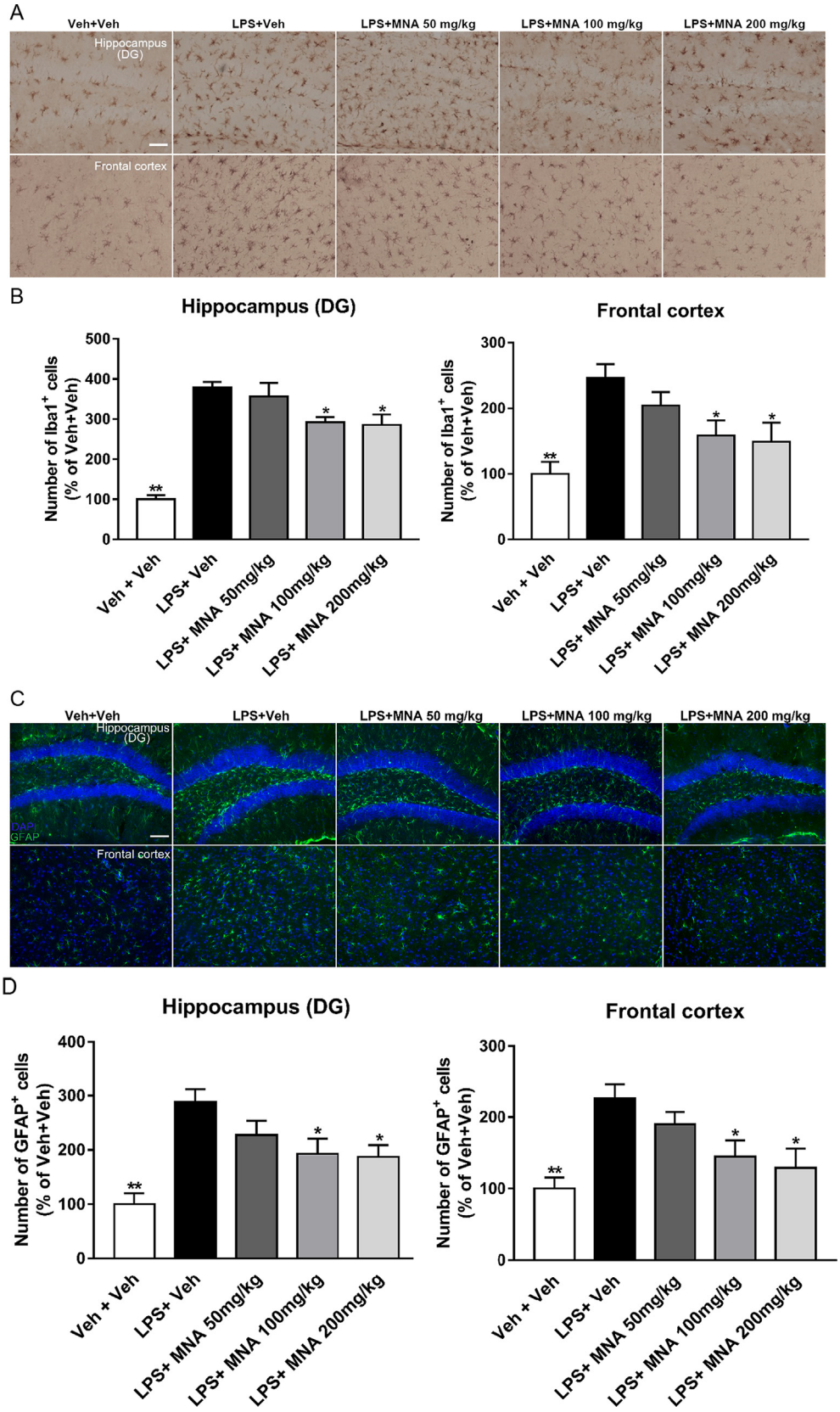

Fig. 4. MNA inhibits LPS-induced glial cells activation in the hippocampus and frontal cortex. (A) Representative IHC microphotographs of microglia activation marker Iba1 in the hippocampus and frontal cortex were shown. (B) The number of Iba1 stained microglia was normalized in the corresponding same area, as the ratio (in percentage) of the Veh + Veh were shown. (C) Representative IF microphotographs of astrocyte activation marker GFAP in the hippocampus and frontal cortex were shown. (D) The number of GFAP stained astrocyte was normalized in the corresponding same area, as the ratio (in percentage) of the Veh + Veh were shown. Values shown were expressed as mean ± SEM; n = 4 mice/group. * $P < 0.05$, ** $P < 0.01$ versus LPS + Veh. Scale bar, 50 μm.

quadrant and the number of escape platform location crossings. LPS injection also caused a significant decline in the discrimination index and increased the latency to enter the shock-free compartment in NOR and Y-maze avoidance tests. In addition, systemic administration of LPS increased neuroinflammation and apoptosis, as clearly shown by increased expressions of NF-κB p65 and inflammatory factors (TNF-α, IL-6), activation of glial cells, increased the number of TUNEL-positive cells, increased the ratio of cleaved caspase-3/pro caspase-3 while

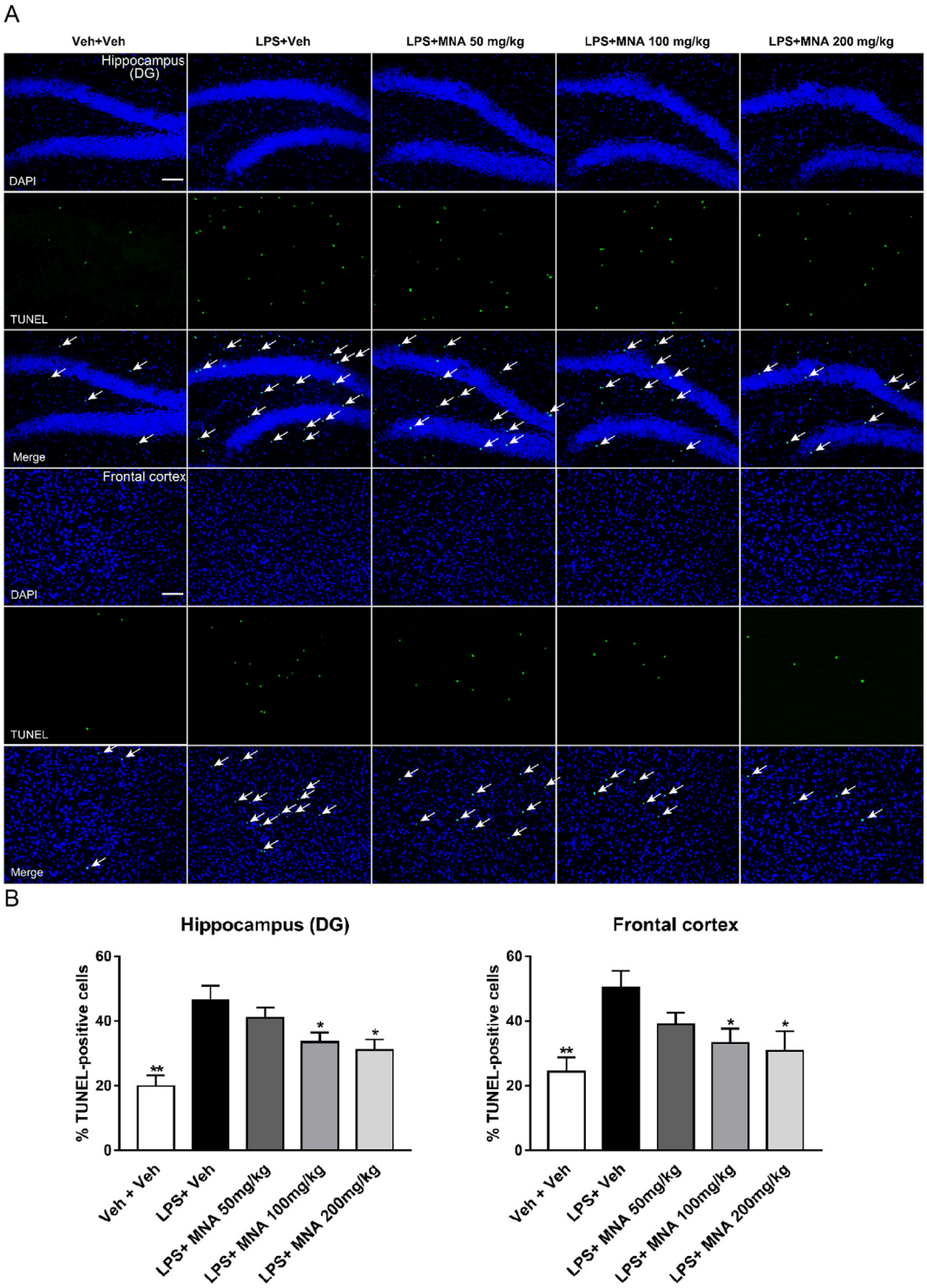

Fig. 5. MNA inhibits LPS-induced apoptosis in the hippocampus and frontal cortex. (A, B) Representative microphotographs of apoptotic cells shown by white arrows and results of percentage (%) of apoptosis in the DG of hippocampus and frontal cortex were shown. (C) Representative IHC microphotographs of neuronal marker NeuN in the DG of hippocampus and frontal cortex were shown. (B) The number of NeuN stained neuron was normalized in the corresponding same area, as the ratio (in percentage) of the Veh + Veh were shown. (E) The expression of pro- and cleaved caspase-3 in the hippocampus and frontal cortex were detected by WB. β-actin was used as a loading control. (F) Caspase-3 activation was shown as the ratio of caspase-3 to pro-caspase-3 of Veh + Veh group. (G) The expression of Bcl-2 and Bax in the hippocampus and frontal cortex were detected by WB. (H) Bcl-2 and Bax were expressed as the ratio of Veh + Veh group. Values shown were expressed as mean ± SEM; n = 4 mice/group. * $P < 0.05$, ** $P < 0.01$ versus LPS + Veh. Scale bar, 50 μm.

decreased the ratio of Bcl-2/Bax in the hippocampus and frontal cortex of mice. Importantly, in this study, MNA treatment (100 or 200 mg/kg) played a protective role and significantly attenuated cognitive deficits and these pathological changes induced by LPS.

It was reported that NA, the precursor of MNA, performed a vital physiological function in the set of biochemical reactions [32,33]. Previous studies have shown that administration of NA can significantly improve cognitive and behavioral function [34,35]. It might play a key

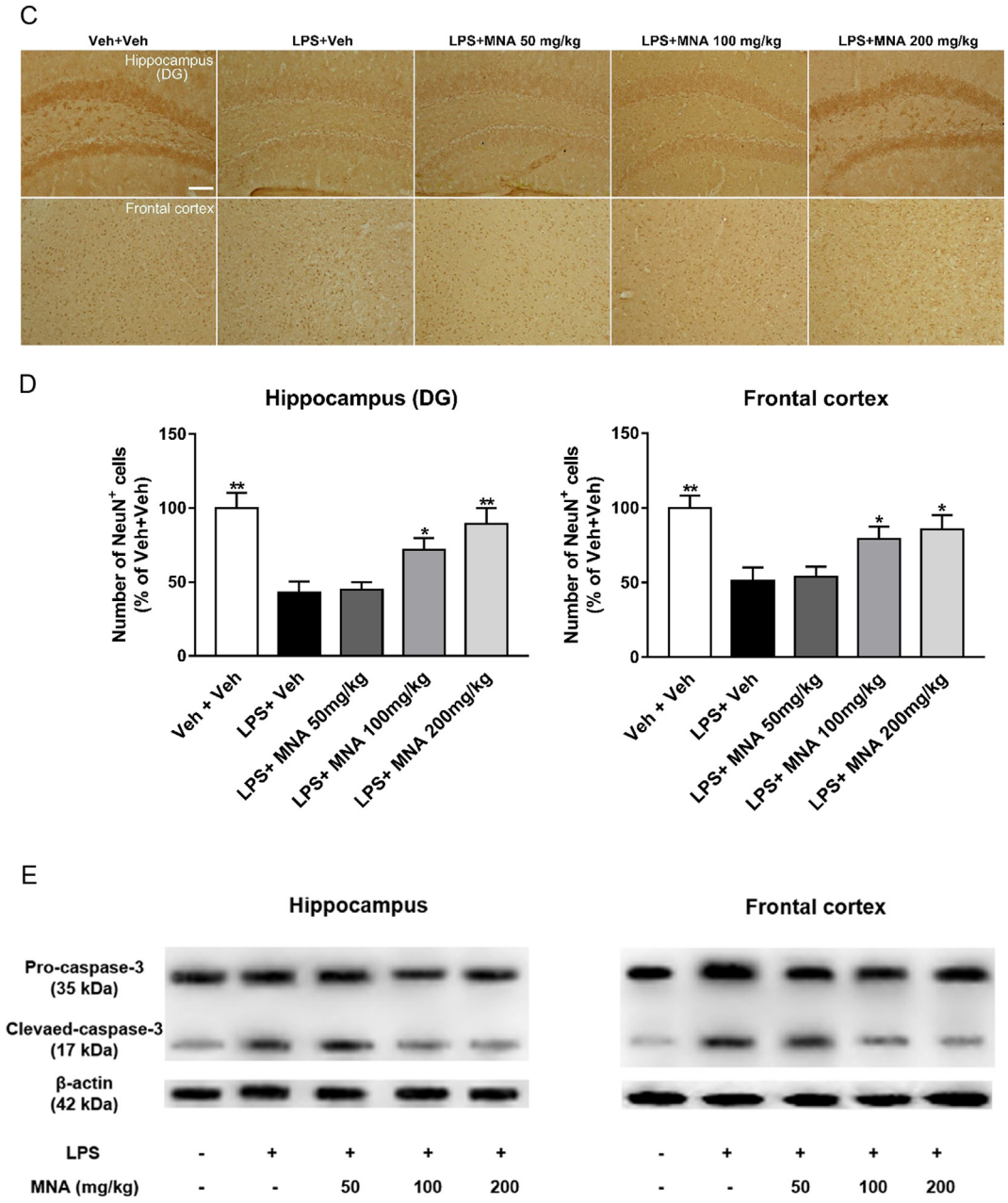

Fig. 5. (*continued*)

role in attenuating the activation of microglia [36] and astrocytes [37]. Moreover, treatment with NA prevents or reduces the activation of neuronal cell death pathways and the following neurodegeneration by inhibiting the caspase-3 and/or PARP-1 over-activation [38]. Some studies reported that MNA, the main metabolite of NA, had neuroprotective effects in diabetes-related brain disorders and hypoxic-ischemic brain damage [17]. Whereas, some other studies showed that MNA led to neurotoxicity [39,40].

NF-κB, an important transcription factor, regulates the expression of a large number of pro-inflammatory mediators including TNF-α and IL-6 [41,42]. Activation of NF-κB signaling promotes apoptosis [43] and inhibition of it defers inflammatory responses [44]. Administration of LPS can activate the NF-κB pathway that plays a significant role in the regulation of neuroinflammation. Previous studies have shown that p65 (also known as RelA), a subunit of the NF-κB transcription factor complex, respond to LPS stimulation [45,46]. MAPK p38, one of the apoptotic pathways, regulates the transcriptional activity of NF-κB p65 in neuroinflammation [47]. More evidences have revealed that MNA can inhibit the p38 MAPK pathway to reduce apoptosis [48]. In this study, we found the high expressions of NF-κB p65 in the hippocampus and frontal cortex of LPS-induced mice, indicating the activation of NF-κB signaling pathway. In contrast, treatment with MNA significantly attenuated these changes of NF-κB p65. Therefore, we speculate that the neuroprotective effects of MNA are associated with NF-κB signaling in the LPS-induced mice.

Microglia and astrocytes are two important sources of inflammatory mediators in the brain [49]. Previous studies reported that aberrant activation of astrocytes and microglia led to the release of inflammatory cytokines, including IL-6 and TNF-α that played an important role in neuronal damage and death [50]. Thus, inhibition of over-activated glial cells may have a neuroprotective effect and ameliorate the severity of AD and other neurological disorders. In this study, LPS administration increased the number of Iba1 and GFAP positive cells in the hippocampus and cortex, indicating the activation of microglia and astrocytes. Treatment with MNA significantly reduced neuroinflammation by suppressing the activation of microglia and

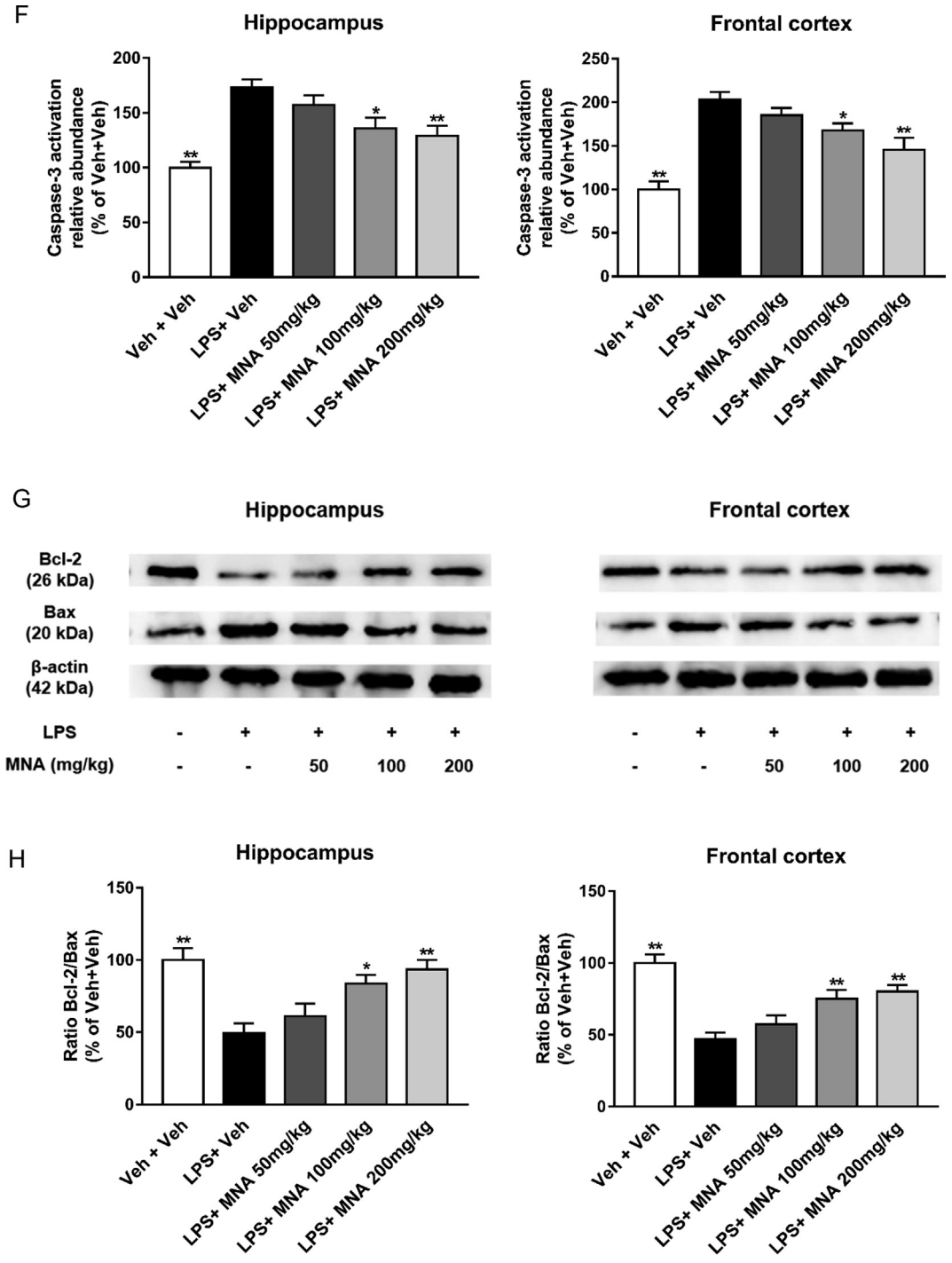

Fig. 5. (*continued*)

astrocytes.

The process of neuronal apoptosis is critical in LPS induced neuroinflammation [51]. Recent studies have reported that caspase-3, cleaved caspase-3 and Bax play a key role in promoting neuronal apoptosis, while Bcl-2 is an antiapoptotic protein [52,53]. Systemic administration of LPS increases the number of apoptotic cells, expression of cleaved caspase-3 and the ratio of Bax/Bcl-2 [30,54,55]. In this study, our results are consistent with previous studies. We found compared to LPS-induced group, there were less TUNEL-positive cells and more NeuN-positive cells in the hippocampus and frontal cortex of MNA-treated mice. The results showed that administration of MNA significantly attenuated LPS-induced neuronal apoptosis and death. Moreover, we found this neuroprotective effect of MNA was involved in the reduction of caspase-3 expression and increase of Bcl-2/Bax ratio. Through this study we suggest that MNA attenuates lipopolysaccharide-induced cognitive deficits via neuroinflammation and apoptosis and might be a novel drug for AD.

5. Conclusion

In conclusion, the present study demonstrates that MNA significantly attenuates LPS-induced cognitive deficits via targeting neuroinflammation and neuronal apoptosis in mice. The neuroprotective effects of MNA are achieved by inhibiting the activation of glial cells and NF-κB signaling. These observations suggest that MNA might be a novel, effective and promising drug for neurodegenerative diseases

such as AD.

Acknowledgements

This work was supported by grants from the National Natural Science Foundation of China (81573413, 81773714 and 81273497 to Hao Hong, 81603113 to Su Su Tang), the “Double First-Class” University Project (CPU2018GF/GY**), and the Fundamental Research Funds for the Central Universities (2632017PT01).

Compliance with Ethical Standards

The National Institutes of Health Guide for the Care and Use of Laboratory Animals (NIH Publications No. 80-23, revised, 1996) was used for the experiments and the procedures were approved by the Animal Care and Use Committee, China Pharmaceutical University.

Declaration of Competing Interest

The authors declare that they have no conflict of interest.

Appendix A. Supplementary material

Supplementary data to this article can be found online at https://doi.org/10.1016/j.intimp.2019.105918.

References

[1] C.R. Abraham, D.J. Selkoe, H. Potter, Immunochemical identification of the serine protease inhibitor alpha 1-antichymotrypsin in the brain amyloid deposits of Alzheimer's disease, Cell 52 (1988) 487–501.
[2] J. Naslund, J. Thyberg, L.O. Tjernberg, C. Wernstedt, A.R. Karlstrom, N. Bogdanovic, et al., Characterization of stable complexes involving apolipoprotein E and the amyloid beta peptide in Alzheimer's disease brain, Neuron 15 (1995) 219–228.
[3] H.Q. Fu, T. Yang, W. Xiao, L. Fan, Y. Wu, N. Terrando, et al., Prolonged neuroinflammation after lipopolysaccharide exposure in aged rats, PLoS ONE 9 (2014) e106331.
[4] D.M. Norden, J.P. Godbout, Review: microglia of the aged brain: primed to be activated and resistant to regulation, Neuropathol. Appl. Neurobiol. 39 (2013) 19–34.
[5] D.M. Bonifati, U. Kishore, Role of complement in neurodegeneration and neuroinflammation, Mol. Immunol. 44 (2007) 999–1010.
[6] S.C. Correia, R.X. Santos, C. Carvalho, S. Cardoso, E. Candeias, M.S. Santos, et al., Insulin signaling, glucose metabolism and mitochondria: major players in Alzheimer's disease and diabetes interrelation, Brain Res. 1441 (2012) 64–78.
[7] S.A. Liddelow, K.A. Guttenplan, L.E. Clarke, F.C. Bennett, C.J. Bohlen, L. Schirmer, et al., Neurotoxic reactive astrocytes are induced by activated microglia, Nature 541 (2017) 481–487.
[8] F. Kazak, G.F. Yarim, Neuroprotective effects of acetyl-l-carnitine on lipopolysaccharide-induced neuroinflammation in mice: involvement of brain-derived neurotrophic factor, NeuroscienceLetters 658 (2017) 32–36.
[9] J.W. Lee, Y.K. Lee, D.Y. Yuk, D.Y. Choi, S.B. Ban, K.W. Oh, et al., Neuro-inflammation induced by lipopolysaccharide causes cognitive impairment through enhancement of beta-amyloid generation, J. Neuroinflammation 5 (2008) 37.
[10] T. Przygodzki, P. Kazmierczak, J. Sikora, C. Watala, 1-methylnicotinamide effects on the selected markers of endothelial function, inflammation and haemostasis in diabetic rats, Eur. J. Pharmacol. 640 (2010) 157–162.
[11] M. Sternak, A. Jakubowski, E. Czarnowska, E.M. Slominska, R.T. Smolenski, M. Szafarz, et al., Differential involvement of IL-6 in the early and late phase of 1-methylnicotinamide (MNA) release in Concanavalin A-induced hepatitis, Int. Immunopharmacol. 28 (2015) 105–114.
[12] T.A. Alston, R.H. Abeles, Substrate specificity of nicotinamide methyltransferase isolated from porcine liver, Arch. Biochem. Biophys. 260 (1988) 601–608.
[13] S. Chlopicki, J. Swies, A. Mogielnicki, W. Buczko, M. Bartus, M. Lomnicka, et al., 1-Methylnicotinamide (MNA), a primary metabolite of nicotinamide, exerts anti-thrombotic activity mediated by a cyclooxygenase-2/prostacyclin pathway, Brit. J. Pharmacol. 152 (2007) 230–239.
[14] Y. Tanaka, S. Kume, H. Araki, J. Nakazawa, M. Chin-Kanasaki, S. Araki, et al., 1-Methylnicotinamide ameliorates lipotoxicity-induced oxidative stress and cell death in kidney proximal tubular cells, Free Radical Biol. Med. 89 (2015) 831–841.
[15] A. Chan, F. Tchantchou, V. Graves, R. Rozen, T.B. Shea, Dietary and genetic compromise in folate availability reduces acetylcholine, cognitive performance and increases aggression: critical role of S-adenosyl methionine, J. Nutr. Health Aging 12 (2008) 252–261.
[16] A.C. Williams, D.B. Ramsden, Nicotinamide homeostasis: a xenobiotic pathway that is key to development and degenerative diseases, Med. Hypotheses 65 (2005) 353–362.
[17] T. Kuchmerovska, I. Shymanskyy, S. Chlopicki, A. Klimenko, 1-methylnicotinamide (MNA) in prevention of diabetes-associated brain disorders, Neurochem. Int. 56 (2010) 221–228.
[18] M. Slomka, E. Zieminska, J. Lazarewicz, Nicotinamide and 1-methylnicotinamide reduce homocysteine neurotoxicity in primary cultures of rat cerebellar granule cells, Acta Neurobiologiae Experimentalis 68 (2008) 1–9.
[19] M. Slomka, E. Zieminska, E. Salinska, J.W. Lazarewicz, Neuroprotective effects of nicotinamide and 1-methylnicotinamide in acute excitotoxicity in vitro, Folia Neuropathol. 46 (2008) 69–80.
[20] M. Ifuku, T. Katafuchi, S. Mawatari, M. Noda, K. Miake, M. Sugiyama, et al., Anti-inflammatory/anti-amyloidogenic effects of plasmalogens in lipopolysaccharide-induced neuroinflammation in adult mice, J. Neuroinflam. 9 (2012) 197.
[21] X. An, F. Shang, RA-XII exerts anti-oxidant and anti-inflammatory activities on lipopolysaccharide-induced acute renal injury by suppressing NF-kappaB and MAPKs regulated by HO-1/Nrf2 pathway, Biochem. Biophys. Res. Commun. 495 (2018) 2317–2323.
[22] F. Chen, A. Ghosh, F. Wu, S. Tang, M. Hu, H. Sun, et al., Preventive effect of genetic knockdown and pharmacological blockade of CysLT1R on lipopolysaccharide (LPS)-induced memory deficit and neurotoxicity in vivo, Brain Behav. Immunity 60 (2017) 255–269.
[23] M.S. Hossain, A. Tajima, S. Kotoura, T. Katafuchi, Oral ingestion of plasmalogens can attenuate the LPS-induced memory loss and microglial activation, Biochem. Biophys. Res. Commun. 496 (2018) 1033–1039.
[24] M.L. Seibenhener, M.C. Wooten, Use of the open field maze to measure locomotor and anxiety-like behavior in mice, J. Visual. Exp.: JoVE (2015) e52434.
[25] M. Antunes, G. Biala, The novel object recognition memory: neurobiology, test procedure, and its modifications, Cognitive Process. 13 (2012) 93–110.
[26] LM. Lueptow, Novel Object Recognition test for the investigation of learning and memory in mice, J. Visual. Exp.: JoVE (2017).
[27] R. Morris, Developments of a water-maze procedure for studying spatial learning in the rat, J. Neurosci. Methods 11 (1984) 47–60.
[28] S.S. Tang, H. Hong, L. Chen, Z.L. Mei, M.J. Ji, G.Q. Xiang, et al., Involvement of cysteinyl leukotriene receptor 1 in A beta(1–42)-induced neurotoxicity in vitro and in vivo, Neurobiol. Aging 35 (2014) 590–599.
[29] S.S. Tang, X.Y. Wang, H. Hong, Y. Long, Y.Q. Li, G.Q. Xiang, et al., Leukotriene D4 induces cognitive impairment through enhancement of CysLT(1)R-mediated amyloid-beta generation in mice, Neuropharmacology 65 (2013) 182–192.
[30] X. Wu, Y.G. Lv, Y.F. Du, M. Hu, M.N. Reed, Y. Long, et al., Inhibitory effect of INT-777 on lipopolysaccharide-induced cognitive impairment, neuroinflammation, apoptosis, and synaptic dysfunction in mice, Prog Neuro-Psychoph. 88 (2019) 360–374.
[31] H.S. Lim, Y.J. Kim, B.Y. Kim, G. Park, S.J. Jeong, The anti-neuroinflammatory activity of tectorigenin pretreatment via downregulated NF-kappaB and ERK/JNK pathways in BV-2 microglial and microglia inactivation in mice with lipopolysaccharide, Front. Pharmacol. 9 (2018) 462.
[32] S.J. Lin, L. Guarente, Nicotinamide adenine dinucleotide, a metabolic regulator of transcription, longevity and disease, Curr. Opin. Cell Biol. 15 (2003) 241–246.
[33] G. Magni, A. Amici, M. Emanuelli, G. Orsomando, N. Raffaelli, S. Ruggieri, Enzymology of NAD+ homeostasis in man, Cell. Mol. Life Sci.: CMLS 61 (2004) 19–34.
[34] M.R. Hoane, S.L. Akstulewicz, J. Toppen, Treatment with vitamin B3 improves functional recovery and reduces GFAP expression following traumatic brain injury in rats, J. Neurotrauma 20 (2003) 1189–1199.
[35] M.R. Hoane, J.L. Pierce, M.A. Holland, G.D. Anderson, Nicotinamide treatment induces behavioral recovery when administered up to 4 hours following cortical contusion injury in the rat, Neuroscience 154 (2008) 861–868.
[36] A.C. Smith, R.C. Holden, S.M. Rasmussen, M.R. Hoane, M.J. Hylin, Effects of nicotinamide on spatial memory and inflammation after juvenile traumatic brain injury, Behav. Brain Res. 364 (2019) 123–132.
[37] M.A. Holland, A.A. Tan, D.C. Smith, M.R. Hoane, Nicotinamide treatment provides acute neuroprotection and GFAP regulation following fluid percussion injury, J. Neurotrauma 25 (2008) 140–152.
[38] A. Ieraci, D.G. Herrera, Nicotinamide inhibits ethanol-induced caspase-3 and PARP-1 over-activation and subsequent neurodegeneration in the developing mouse cerebellum, Cerebellum 17 (2018) 326–335.
[39] T. Fukushima, A. Kaetsu, H. Lim, M. Moriyama, Possible role of 1-methylnicotinamide in the pathogenesis of Parkinson's disease, Exp. Toxicol. Pathol. 53 (2002) 469–473.
[40] Y. Mori, A. Sugawara, M. Tsuji, T. Kakamu, S. Tsuboi, H. Kanda, et al., Toxic effects of nicotinamide methylation on mouse brain striatum neuronal cells and its relation to manganese, Environ. Health Preventive Med. 17 (2012) 371–376.
[41] S. Umesalma, G. Sudhandiran, Differential inhibitory effects of the polyphenol ellagic acid on inflammatory mediators NF-kappaB, iNOS, COX-2, TNF-alpha, and IL-6 in 1,2-dimethylhydrazine-induced rat colon carcinogenesis, Basic Clin. Pharmacol. Toxicol. 107 (2010) 650–655.
[42] J.H. Won, J.Y. Kim, K.J. Yun, J.H. Lee, N.I. Back, H.G. Chung, et al., Gigantol isolated from the whole plants of Cymbidium goeringii inhibits the LPS-induced iNOS and COX-2 expression via NF-kappaB inactivation in RAW 264.7 macrophages cells, PlantaMedica 72 (2006) 1181–1187.
[43] M. Khan, Y.B. Im, A. Shunmugavel, A.G. Gilg, R.K. Dhindsa, A.K. Singh, et al., Administration of S-nitrosoglutathione after traumatic brain injury protects the neurovascular unit and reduces secondary injury in a rat model of controlled cortical impact, J. Neuroinflammation 6 (2009) 32.
[44] T. Lawrence, D.W. Gilroy, P.R. Colville-Nash, D.A. Willoughby, Possible new role for NF-κB in the resolution of inflammation, NatureMedicine 7 (2001) 1291.

[45] A. Hoffmann, D. Baltimore, Circuitry of nuclear factor κB signaling, Immunol. Rev. 210 (2006) 171–186.
[46] A.R. Vasconcelos, L.M. Yshii, T.A. Viel, H.S. Buck, M.P. Mattson, C. Scavone, et al., Intermittent fasting attenuates lipopolysaccharide-induced neuroinflammation and memory impairment, J. Neuroinflam. 11 (2014) 85.
[47] R.N. Saha, M. Jana, K. Pahan, MAPK p38 regulates transcriptional activity of NF-κB in primary human astrocytes via acetylation of p65, J. Immunol. 179 (2007) 7101–7109.
[48] X. Xie, H. Liu, Y. Wang, Y. Zhou, H. Yu, G. Li, et al., Nicotinamide N-methyltransferase enhances resistance to 5-fluorouracil in colorectal cancer cells through inhibition of the ASK1-p38 MAPK pathway, Oncotarget 7 (2016) 45837.
[49] F. Zhang, J.-G. Zhang, W. Yang, P. Xu, Y.-L. Xiao, H.-T. Zhang, 6-Gingerol attenuates LPS-induced neuroinflammation and cognitive impairment partially via suppressing astrocyte overactivation, Biomed. Pharmacother. 107 (2018) 1523–1529.
[50] G. Luo, Y. Huang, D. Mo, N. Ma, F. Gao, L. Song, et al., Tyrosol attenuates pro-inflammatory cytokines from cultured astrocytes and NF-kappaB activation in in vitro oxygen glucose deprivation, Neurochem. Int. 121 (2018) 140–145.
[51] Y. Song, J. Shen, Y. Lin, J. Shen, X. Wu, Y. Yan, et al., Up-regulation of podoplanin involves in neuronal apoptosis in LPS-induced neuroinflammation, Cell. Mol. Neurobiol. 34 (2014) 839–849.
[52] C. Huang, C. Wen, M. Yang, D. Gan, C. Fan, A. Li, et al., Lycopene protects against t-BHP-induced neuronal oxidative damage and apoptosis via activation of the PI3K/Akt pathway, Mol. Biol. Rep. 1–11 (2019).
[53] T. Wang, Y. Cheng, H. Han, J. Liu, B. Tian, X. Liu, miR-194 accelerates apoptosis of Aβ1–42-transduced hippocampal neurons by inhibiting Nrn1 and decreasing PI3K/Akt signaling pathway activity, Genes 10 (2019) 313.
[54] Y.J. Lee, D.Y. Choi, I.S. Choi, K.H. Kim, Y.H. Kim, H.M. Kim, et al., Inhibitory effect of 4-O-methylhonokiol on lipopolysaccharide-induced neuroinflammation, amyloidogenesis and memory impairment via inhibition of nuclear factor-kappaB in vitro and in vivo models, J. Neuroinflam. 9 (2012) 35.
[55] J. Shi, Y. Zhao, Y. Wang, W. Gao, J. Ding, P. Li, et al., Inflammatory caspases are innate immune receptors for intracellular LPS, Nature 514 (2014) 187–192.